

1 Using citizen science reports to define the equatorial
2 extent of auroral visibility

N. A. Case^{1,2,3}, E. A. MacDonald^{1,2} and R. Viereck⁴

¹New Mexico Consortium, Los Alamos,
New Mexico, USA

²NASA Goddard Space Flight Center,
Greenbelt, Maryland, USA

³Department of Physics, Lancaster
University, Lancaster, UK

⁴NOAA Space Weather Prediction
Center, Boulder, Colorado, USA

Abstract. An aurora may often be viewed hundreds of kilometers equatorward of the auroral oval owing to its altitude. As such, the NOAA Space Weather Prediction Center (SWPC) Aurora Forecast product provides a “view-line” to demonstrate the equatorial extent of auroral visibility, assuming that it is sufficiently bright and high in altitude. The view-line in the SWPC product is based upon the latitude of the brightest aurora, for each hemisphere, as specified by the real-time Oval Variation, Assessment, Tracking, Intensity, and Online Nowcasting (OVATION) Prime (2010) aurora precipitation model. In this study, we utilize nearly 500 citizen science auroral reports to compare with the view-line provided by an updated SWPC aurora forecast product using auroral precipitation data from OVATION Prime (2013). The citizen science observations were recorded during March and April 2015 using the Aurorasaurus platform and cover one large geomagnetic storm and several smaller events. We find that this updated SWPC view-line is conservative in its estimate and that the aurora is often viewable further equatorward than is indicated by the forecast. By using the citizen reports to modify the scaling parameters used to link the OVATION Prime (2013) model to the view-line, we produce a new view-line estimate that more accurately represents the equatorial extent of visible aurora. An OVATION Prime (2013) energy-flux-based equatorial boundary view-line is also developed and is found to provide the best overall agreement with the citizen science reports, with an accuracy of 91%.

1. Introduction

25 Knowing when, and from where, an aurora will be visible is an aspect of space weather
26 science that interests researchers and the general public alike. In fact, one of the only ways
27 the general public can experience space weather first-hand is to witness an aurora and
28 there is a small, but growing, tourism industry catering to people who want to do just that.
29 Several auroral precipitation models, based either upon current solar wind conditions or
30 estimated real-time geomagnetic indices, exist which can aid in this regard by predicting
31 the size and location of the auroral oval (e.g. *Spiro et al.* [1982]; *Hardy et al.* [1985, 1989];
32 *Roble and Ridley* [1987]; *Zhang and Paxton* [2008]; *Newell et al.* [2010b, 2014]; *Mitchell*
33 *et al.* [2013]).

34 Oval Variation, Assessment, Tracking, Intensity, and Online Nowcasting (OVATION)
35 Prime is one such auroral precipitation model [*Newell et al.*, 2010b, 2014]. This particular
36 model is driven by the rate of delivery of interplanetary magnetic flux to Earth's magne-
37 topause as parameterized by the $d\Phi_{MP}/dt$ magnetospheric coupling function [*Newell et*
38 *al.*, 2007]. This coupling function is in turn dependent upon the solar wind conditions as
39 measured at Earth's first Lagrangian orbital point (L1), located approximately 1 million
40 miles (1.5 million kilometers) upstream on the Sun-Earth line. Since the coupling function
41 is solar-wind driven, the model can be run in real-time using upstream solar wind data.
42 This real-time run ability makes the model especially useful for space weather forecasting
43 as it typically provides a 30-40 min forecast of the overall size and intensity of the auroral
44 ovals.

45 When calculating the auroral precipitation, OVATION Prime accounts for several dif-
46 ferent auroral types (i.e. diffuse aurora, monoenergetic, broadband, and ion), seasonal
47 variations, and the magnetic latitude (MLAT) and magnetic local time (MLT) of each
48 of its modeled bins (which are 0.5° in MLAT by 0.25° , or 1 min, in MLT in size). All
49 of which ensures that it is often more accurate at modeling the auroral oval than other
50 real-time models [*Newell et al.*, 2014; *Lane et al.*, 2015] and can reliably predict when an
51 aurora will be visible [*Machol et al.*, 2012].

52 The original version of the model, referred to as OVATION Prime (2010) [*Newell et*
53 *al.*, 2010b], has been further developed to increase its accuracy at larger geomagnetic
54 activity levels (particularly in the Kp 5+ to 8+ range) and to reduce the noise between
55 neighboring bins. This latest version of the model is known as OVATION Prime (2013)
56 [*Newell et al.*, 2014]. OVATION Prime (2010) is subsequently referred to as OP10 and
57 OVATION Prime (2013) as OP13 throughout.

58 NOAA’s Space Weather Prediction Center (SWPC) has been running OP10 in real-
59 time since 2011. As described in the following Methods section, SWPC uses the model
60 to provide auroral precipitation data for their public-orientated aurora forecast product.
61 Included in this forecast product is an estimate of the most equatorward latitude, for both
62 hemispheres, from which an aurora might be visible, known as a “view-line”.

63 Whilst both OP10 and OP13 have been validated and found to provide reasonable
64 estimates of the location and intensity of the aurora (e.g. *Machol et al.* [2012]; *Newell et*
65 *al.* [2014]; *Lane et al.* [2015]), no extensive testing has yet been performed on the accuracy
66 of the SWPC forecast product or the location of the view-line.

67 In this study, nearly 500 citizen science reports, collected by the Aurorasaurus project
68 [*MacDonald et al.*, 2015], are evaluated and compared against an updated version of the
69 SWPC view-line which is based on OP13 data. Furthermore, the reports are then used to
70 create an observationally based Aurorasaurus view-line and to test an auroral equatorial
71 boundary based view-line.

72 We note one previous, related, effort by *Gartlein and Moore* [1951] showed that a decade
73 long network of dedicated observers could track the southern extent of the aurora over
74 North America. The work contained herein can be seen as an extension to this, in which
75 real-time, globally-distributed, reports are compared to modern models for auroral extent,
76 something that was not possible for *Gartlein and Moore* [1951].

2. Methods

77 As previously mentioned, SWPC uses the real-time data output from OP10 to drive its
78 aurora forecast product. The model output is converted from geomagnetic coordinates
79 into geographic and is then resampled into an array of 1024 bins in longitude and 512 in
80 latitude (i.e. each bin is approximately 0.35° in latitude and longitude).

81 The precipitating energy flux of each auroral type, excluding ion precipitation, is
82 summed and converted into an empirical estimate of the “probability of visible aurora”.
83 The ion portion of energy flux is excluded since, generally, ion precipitation does not
84 contribute to the visible aurora in the traditional auroral oval. We note that ion (or pro-
85 ton) precipitation does, however, contribute to sub-visual auroral structures, including
86 proton aurora [*Donovan et al.*, 2012] and Stable Auroral Red (SAR) arcs that form at
87 mid-latitudes [*Baumgardner et al.*, 2008].

88 As shown in Equation 1, the purely empirical conversion between the summed precip-
 89 itation energy flux, Σj (measured in $\text{erg cm}^{-2} \text{s}^{-1}$), and the percentage probability of
 90 visible aurora, $P(A)$, involves simply scaling the energy flux for each bin and adding an
 91 offset.

$$P(A) = 10 + 8\Sigma j \quad (1)$$

92 The resultant probability values are then smoothed, small values are clipped, and an
 93 upper limit of 100% is applied. A text file containing these gridded $P(A)$ values is made
 94 available to download in real-time from the SWPC website.

95 Additionally since an aurora can be viewed, especially during high activity, hundreds
 96 of kilometers equatorward of the visible auroral oval, a coarse “view-line” is estimated.
 97 The view-line indicates the most equatorward latitude, for a range of longitudes, from
 98 which an observer might be able to see an aurora (i.e. at latitudes poleward of this line,
 99 an aurora should be visible).

100 The SWPC view-line is determined independently for both hemispheres. Each of the
 101 1024 geographic longitudinal arrays (spaced at 0.35° intervals) are split by hemisphere,
 102 and the maximum probability of visible aurora ($P(A)_{max}$) in that longitudinal hemispheric
 103 array is determined. The latitude of the most equatorward bin, in that array, containing
 104 this maximum probability is then found ($\phi_{P(A)_{max}}$).

105 As shown in Equation 2, $\phi_{P(A)_{max}}$ is scaled equatorward, by a factor dependent upon
 106 $P(A)_{max}$, to give the view-line latitude (ϕ_{VL}^{SWPC}) for that specific longitude and hemisphere.

$$\phi_{VL}^{SWPC} = \phi_{P(A)_{max}} \pm \left(\frac{P(A)_{max}}{20} + 3 \right) \quad (2)$$

107 Note that the \pm sign is required to scale the latitude equatorward for both hemispheres
108 (when using a $\pm 90^\circ$ range of latitudes). A five element smoothing function is applied to
109 the view-line and the view-line is then clipped at the day/night terminators.

110 In this study, the official SWPC aurora forecast product has been updated so that it uses
111 OP13 data, rather than OP10. Whilst this may sometimes result in a slightly different
112 view-line than is provided by the official product on the SWPC website, it should ensure
113 that the output is more accurate - especially during strong auroral displays. No other
114 changes to the SWPC product have been made. This updated, OP13 version of the SWPC
115 aurora forecast product is herein referred to as the “updated SWPC product”.

116 An example of the OP13 output and the corresponding updated SWPC product, in-
117 cluding the view-line determined using Equation 2, is shown in Figure 1.

3. Citizen Science Data

118 Used in this study are 494 Aurorasaurus citizen science reports which were recorded
119 during March and April 2015. These months were selected because they encompassed sev-
120 eral periods of high geomagnetic activity, including a severe G4-level storm on the NOAA
121 geomagnetic storm scale [*Poppe, 2000*]. During such intense geomagnetic activity the
122 number of aurora observations, perhaps unsurprisingly, increases significantly allowing for
123 larger statistical analyses [*Case et al., 2015b*]. Covering larger storms is also particularly
124 useful since most auroral models lack observational data during periods of high activity
125 (owing to their relative rarity).

126 Aurorasaurus has been collecting a standardized set of auroral visibility reports, made
127 by the general public, since November 2014. The reports are submitted via the project’s
128 website and mobile apps, and are also sourced from Twitter. These reports, which act

129 as “ground-truths” for auroral visibility, all contain a timestamp and location, and many
130 contain extra details about the sighting such as the color, structure, or activity of the
131 aurora. Some will also include a photograph of the sighting.

132 The Aurorasaurus reports are grouped into two primary categories, positive and nega-
133 tive, identifying if the observer was able to see an aurora. Positive reports, which make
134 up 85% of the reports in this case study, are composed of reports submitted directly
135 to Aurorasaurus, known as positive sightings, and reports posted on Twitter. Twitter
136 reports, which can also provide useful information about auroral activity [*Case et al.*,
137 2015a], are found using keyword searching, verified by Aurorasaurus users as real-time
138 aurora sightings, and then manually verified by Aurorasaurus team members (see *Mac-*
139 *Donald et al.* [2015] for further details). Once verified, these Twitter reports are known
140 as verified tweets.

141 There are also two types of negative reports: those that did not see the aurora because
142 their view was obstructed (e.g. cloud cover, physical obstacles/terrain, or light pollution)
143 and those whose view was not obstructed, hence, an aurora was simply not visible at that
144 location. It is the latter type of negative report that is of interest in this study, since
145 the view-line does not take into account local conditions. Therefore, the negative reports
146 have been filtered to those that indicated a clear, unobstructed, view of the night sky.

147 Furthermore, all reports submitted directly to Aurorasaurus, either through its web-
148 site or mobile apps, are checked for obvious data integrity issues. For example, reports
149 spanning more than three hours (usually a result of the user selecting an incorrect end
150 time) are filtered out, as are any reports submitted by the same user within the same time
151 period (i.e. multiple submissions of the same report).

4. Results

152 Plotted in the top panel of Figure 2, are the absolute magnetic latitudes of the 494
 153 Aurorasaurus reports submitted during March and April 2015, grouped into 0.5° intervals.
 154 The stacked color bars indicate the number of each type of report in each interval. Negative
 155 reports (of which there are 74) are colored red, positive sightings(240) green and verified
 156 tweets (180) blue. The positive sightings and verified tweets collectively span from 43.8°
 157 to 73.2° in absolute magnetic latitude, with a median latitude of 58.6° .

158 In the middle panel of Figure 2, the reports are grouped by their estimated local time
 159 (LT) in 30 minute bins. The term “estimated” is used since all reports are actually
 160 recorded in UT, and so the local time of the report is determined using this UT value and
 161 the report’s longitude. Adjustments for daylight savings time are made when appropriate.
 162 The positive sightings and verified tweets collectively span from approximately 19:00 to
 163 07:00 LT, with the median start time of 22:45 LT.

164 In the bottom panel of Figure 2, the reports are grouped by the corresponding Kp
 165 value at the start of the report. The Kp index [*Bartels et al.*, 1939], is a 3-hourly quasi-
 166 logarithmic index describing the global geomagnetic activity level, ranging from 0 to 9,
 167 and is provided by NASA’s OMNIweb data archive. The corresponding Kp values for the
 168 Aurorasaurus reports span from 0 to 7, with a median value of 5.

4.1. Updated SWPC view-line

169 To investigate the accuracy of the updated SWPC view-line, the difference in latitude
 170 between each report ($|\phi_{\text{rep}}|$) and the view-line ($|\phi_{\text{VL}}^{\text{SWPC}}|$) is determined. Reports that are
 171 equatorward of the view-line result in a positive difference whilst those that are poleward
 172 result in a negative difference. A histogram of these differences is shown in Figure 3.

173 We note that some of the reports could not be compared with the updated SWPC view-
 174 line which was generally the result of invalid solar wind data resulting in no valid OP13
 175 output.

176 The median difference of the positive reports, which includes positive sightings and
 177 verified tweets, is $+1.26^\circ$ (approximately 140km equatorward). Though since the view-
 178 line is an estimate of the most equatorward latitude from which an observer might see
 179 the aurora, in this study we are primarily interested in those positive reports that occur
 180 equatorward of the view-line (i.e. $|\phi_{\text{rep}}| < |\phi_{\text{VL}}^{\text{SWPC}}|$). When filtering to those reports,
 181 which account for 62.0% of the total positive reports, the median difference is $+3.70^\circ$ (or
 182 approximately 400km equatorward).

183 The overall accuracy (ACC) of the updated SWPC view-line can be determined from
 184 the ratio of the sum of the true positives (ΣTP) and true negatives (ΣTN) to the total
 185 number of reports (ΣR) [Machol *et al.*, 2012]. Specifically;

$$\text{ACC} = \frac{\Sigma\text{TP} + \Sigma\text{TN}}{\Sigma R} \quad (3)$$

186 where a true positive is a positive report that occurred on, or poleward of, the view-line
 187 and a true negative is a negative report that occurred equatorward of the view-line. For
 188 the updated SWPC view-line, $\Sigma\text{TP} = 108$, $\Sigma\text{TN} = 33$ and $\Sigma R = 321$, thus, the accuracy
 189 is found to be 43.9%.

4.2. Aurorasaurus view-line

190 The validity of the SWPC view-line coefficients (Equation 2) can be tested by replacing
 191 $\phi_{\text{VL}}^{\text{SWPC}}$ with the latitudes of the positive reports (ϕ_{rep}). Then, by rearranging Equation 2
 192 and plotting the difference between the positive reports and the location of maximum

193 probability of visible aurora (i.e. $|\phi_{P(A)max}| - |\phi_{rep}|$) as a function of $P(A)_{max}$, the
 194 coefficients of the fit can be determined.

195 Again, we are interested in the most equatorward location of the visible aurora, rather
 196 than just an average. As such, a least squares fit through all the data is not the most
 197 appropriate fit to make. Instead a least squares fit through the maximum difference (i.e.
 198 the largest value of $|\phi_{P(A)max}| - |\phi_{rep}|$) in 5° degree intervals is computed. As shown in
 199 Figure 4, the line of best fit takes the form: $|\phi_{P(A)max}| - |\phi_{rep}| = (0.063 \pm 0.028) P(A)_{max} +$
 200 (8.27 ± 1.67) . A linear fit is assumed owing to the linear relationship in Equation 2. The
 201 Pearson's correlation coefficient for this linear relation is $r = 0.48$.

202 A view-line determined using the Aurorasaurus positive reports and $P(A)_{max}$ can now
 203 be created and is given in Equation 4:

$$\phi_{VL}^{AS} = \phi_{P(A)max} \pm \left(\frac{P(A)_{max}}{16} + 8 \right) \quad (4)$$

204 In Figure 5, the difference between the reports and this new Aurorasaurus view-line
 205 (ϕ_{VL}^{AS}) are shown in a similar form to Figure 3. The median difference of the positive reports
 206 is now -4.55° (500km poleward) and 92.7% of the positive reports are poleward of the
 207 view-line. The accuracy of the view-line, as defined in Equation 3, is 90.1% ($\Sigma TP = 240$,
 208 $\Sigma TN = 23$ and $\Sigma R = 292$).

4.3. Equatorial Boundary view-line

209 The updated SWPC view-line (ϕ_{VL}^{SWPC}) and the Aurorasaurus one based upon it (ϕ_{VL}^{AS}),
 210 are determined using the latitude of the peak intensity of the aurora ($\phi_{P(A)max}$). This
 211 leads, at times, to unrealistic situations wherein the view-line lies within a wide auroral
 212 oval (see Figure 1). A view-line based upon the latitude of the equatorial boundary of

213 the aurora, rather than the latitude of the peak intensity, is therefore investigated. In the
 214 following, the equatorial boundary is defined as the most equatorward latitude at which
 215 $P(A) \geq 18\%$, which equates to $\Sigma j \geq 1 \text{ erg cm}^{-2} \text{ s}^{-1}$ (c.f. *Machol et al.* [2012] who cite
 216 this threshold as approximately corresponding to visible aurora).

217 In Figure 6, the difference between the latitude of the Aurorasaurus reports (ϕ_{rep})
 218 and the equatorial boundary of the OP13 modeled auroral oval (ϕ_{EB}) is investigated.
 219 The median difference for all positive reports is 0.62° (approximately 70km equatorward)
 220 and when filtering to reports where $|\phi_{\text{rep}}| < |\phi_{\text{EB}}|$ the median difference is $+3.06^\circ$ (or
 221 approximately 350km equatorward). The accuracy of using just the equatorial boundary
 222 as the view-line is 49.7%.

223 The difference in latitude between the positive reports and the equatorial boundary,
 224 as a function of $P(A)_{\text{max}}$, is shown in Figure 7. The figure takes a similar form to Fig-
 225 ure 4, and the line of best fit through the maximums is found to be: $|\phi_{\text{EB}}| - |\phi_{\text{rep}}| =$
 226 $(0.00 \pm 0.03) P(A)_{\text{max}} + (7.65 \pm 2.06)$. Using this fit, a view-line based upon the relation-
 227 ship between the positive reports and the equatorial boundary can be determined and is
 228 given in Equation 5.

$$\phi_{\text{VL}}^{\text{EB}} = \phi_{\text{EB}} \pm 8 \quad (5)$$

229 In Figure 8, the difference between the reports and this new equatorial boundary based
 230 view-line ($\phi_{\text{VL}}^{\text{EB}}$) are shown in a similar form to Figure 3. The median difference of the
 231 positive reports is 7.74° (850 km poleward) and 95.0% of the positive reports are poleward
 232 of the view-line. The accuracy of this view-line is 91.2% ($\Sigma\text{TP} = 246$, $\Sigma\text{TN} = 12$ and
 233 $\Sigma R = 283$).

234 The results of comparing the Aurorasaurus citizen science reports with each of the view-
235 lines previously discussed (i.e. the updated SWPC view-line, the Aurorasaurus view-line,
236 and the Equatorial Boundary based view-line) are summarized in Table 1.

5. Discussion

237 An aurora “view-line” estimates the most equatorial latitude from which an observer
238 might see an aurora based upon the current (or predicted) auroral oval size and strength.
239 Since the visible aurora can reach over 400km in altitude [*Kataoka et al.*, 2013], a simple
240 estimate places this view-line in the region of $9 - 10^\circ$ in latitude from the auroral oval.

241 Of course, such a basic approach neglects several factors including the width of the
242 auroral oval (which can span several degrees in latitude), the total aurora precipitation flux
243 (which can affect its luminosity) and the type of aurora. In the early evening, for example,
244 the aurora typically consists of quiet arcs that do not extend far in latitude. Therefore,
245 the viewing range will likely be reduced in those early evening sector longitudes. Similarly,
246 the patchy or pulsating aurora in the dawn sector may not have the large vertical extent
247 required to be observed from large distances away. It is usually the pre-midnight/midnight
248 sector that has bright aurora, with large vertical rays, and the spread in altitude required
249 to observe aurora from large distances.

250 As shown in the middle panel of Figure 2, the majority of the Aurorasaurus reports take
251 place in the pre-midnight local time sector. Thus, perhaps unsurprisingly, the majority
252 of positive reports occur most often when the aurora is likely to be at its brightest and
253 visible from large distances away. Of course, the pre-midnight hours are also the most
254 sociable for citizen scientist observers to be out “aurora-hunting”. Future work should

255 attempt to account for local time when determining the location of the view-line, but such
256 work is beyond the scope of this initial case study.

257 As shown in Equation 2, to try to account for some of these complicating factors,
258 SWPC provides an equatorward view-line estimate that is based upon both the maximum
259 intensity of the aurora (or, rather, the maximum probability of visible aurora) and the
260 location at which this occurs, as determined by OP10. Though in this study, SWPC's
261 estimate was updated by using OP13 as the auroral precipitation data source.

262 It should be expected that if this estimate is performing well, almost all of the Auro-
263 rasaurus positive reports (i.e. positive sightings and verified tweets) would be poleward of
264 this view-line. Of course, we might expect that some positive reports would be equator-
265 ward, though, owing to factors not accounted for in OP13, such as a sudden brightening
266 of the aurora (e.g., the result of a substorm), the observer's altitude, or their camera
267 sensitivity.

268 Plotted in Figure 3 are the differences between the Aurorasaurus reports and the up-
269 dated SWPC view-line. The distribution of the histogram showed that 62% of the positive
270 reports were equatorward of the view-line with a median difference of $+3.70^\circ$, or approx-
271 imately 400km equatorward. These results suggest that the updated SWPC view-line is
272 somewhat conservative. Additionally, the accuracy of the view-line (as determined using
273 Equation 3) was poor at 43.9%.

274 It is important to note, however, that the large majority (85%) of the Aurorasaurus
275 reports are positive (i.e. positive sightings or verified tweets). This is perhaps to be
276 expected since citizen scientists are more likely to be motivated to report their observations
277 when the outcome is favorable (i.e. they saw an aurora) (c.f. *Sequeira et al.* [2014]).

278 Unfortunately, however, this positive reporting skew may be considered as a form of
279 sampling bias that may affect the determined view-line accuracy since we are, in particular,
280 lacking in “true negatives” (i.e. as predicted, an observer equatorward of the view-line was
281 unable to see an aurora) and “false positives” (i.e. an observer poleward of the view-line,
282 with clear skies and an unobstructed view, was unable to see an aurora).

283 Additionally, reports made by citizen scientists are generally made near areas of fairly
284 high population. As such, and as shown in the top panel of Figure 2, the majority of the
285 Aurorasaurus reports are most likely from the equatorial edge of a visible aurora. Whilst
286 this is actually quite useful when determining the equatorial extent of a visible aurora, it
287 does mean that there is a bias toward lower latitude values when determining the overall
288 accuracy of a view-line (i.e. there are less “true positives” at latitudes greater than the
289 view-line latitude - even though an aurora would, indeed, be visible from there).

290 To further compare the view-line with the positive reports, the difference in latitude
291 between them was plotted against the maximum probability of visible aurora in Figure 4.
292 We note that the large grouping at $P(A)_{max} = 100\%$, which contained around 30% of the
293 positive reports, is simply an artifact of the conversion of energy flux into a percentage
294 (which, clearly, has an upper bound). Since we were specifically interested in comparing
295 the observations with the updated SWPC view-line, the visibility percentage was chosen
296 in this case study. However, further work could investigate the relationship between the
297 OP13 modeled energy flux, rather than the SWPC percentage values, and the latitude
298 from which an aurora was visible.

299 Additionally, when determining the distance between the reports and the view-line, it
300 is simply the distance along the same longitude that is calculated. In reality, though,

301 an aurora may be visible from a location with a different longitude (i.e. an aurora may
302 be visible to the North-East rather than due North). The calculated distance between
303 the reports and the view-line may, therefore, not accurately represent the actual distance
304 between the reporter and the closest location of the view-line.

305 A line of best fit through these data provides observationally derived coefficients that can
306 replace those in Equation 2. Since a view-line is the most equatorward location from which
307 the aurora might be seen, the line of best fit was plotted through the maximum differences.
308 The original view-line coefficients were then replaced with these fitting parameters, to
309 produce an observationally based Aurorasaurus view-line, in Equation 4. We note that
310 there is some considerable spread in the data, which results in large uncertainties in
311 the fitting parameters. Indeed, the correlation coefficient for this fit is moderate-poor,
312 $r = 0.48$, which further demonstrates the uncertainty in this relationship. Using additional
313 data to compute this fit may help to reduce such uncertainties.

314 The reports were then compared with this Aurorasaurus view-line (ϕ_{VL}^{AS}) in Figure 5.
315 This comparison demonstrated that 92.7% of the positive reports were poleward of the
316 view-line and the median difference was -4.55° (500km poleward). The accuracy of this
317 modified view-line is 90.1% (more than double the updated SWPC view-line accuracy).

318 Both the updated SWPC view-line and the Aurorasaurus view-line scale the location of
319 the maximum auroral visibility equatorward by some factor, since this is the most likely
320 location of aurora visible directly overhead. However, it is quite possible that the aurora
321 may also be visible overhead at latitudes further equatorward than this (for example, the
322 maximum visibility may be 100% at one latitude but still 90% several degrees equatorward
323 of this). As such, the location of the reports were also compared with the location of the

324 auroral equatorial boundary in Figure 6. The location of the equatorial boundary was
 325 defined as the most equatorward latitude at which $P(A) \geq 18\%$.

326 The median difference for the positive reports was 0.62° (approximately 70km equa-
 327 torward). When filtering to only those reports equatorward of the equatorial boundary
 328 the median difference was $+3.06^\circ$ (approximately 350km equatorward). The accuracy of
 329 using just the equatorial boundary as a view-line was found to be 49.7%.

330 Of course, it is expected that there should be some scaling involved, just as there is
 331 with the updated SWPC and Aurorasaurus view-lines. To determine the appropriate
 332 scaling factors, the latitude difference between the positive reports and the equatorial
 333 boundary was plotted against the maximum probability of visible aurora in Figure 7. The
 334 coefficients of the fit then provided the scaling needed to compute an equatorial boundary
 335 based view-line (ϕ_{VL}^{EB}) - as shown in Equation 5.

336 Interestingly, there is found to be no dependence on $P(A)_{max}$, rather ϕ_{VL}^{EB} is just the
 337 location of the equatorial boundary (ϕ_{EB}) scaled equatorward by 8° . This suggests that
 338 location of the equatorial boundary may itself scale based upon $P(A)_{max}$ (i.e. ϕ_{EB} moves
 339 equatorward as $P(A)_{max}$ increases) which is, perhaps, unsurprising.

340 The reports were then compared to the equatorial boundary based view-line. This
 341 comparison shows that 95.0% of the positive reports were poleward of the view-line and
 342 that the median difference was -7.74° (850 km poleward). The accuracy was found to
 343 be slightly higher than the Aurorasaurus view-line (91.2%) and considerably higher than
 344 the updated SWPC view-line (43.9%).

345 During the aforementioned comparisons, the number of reports used varies from the
 346 total number shown in Figure 2. This is due to some reports being recorded at longitudes

347 with no associated view-line, e.g. the observation was at dusk/dawn and the view-line had
348 been trimmed from that longitude due to the presence of the day/night terminator or, in
349 the case of the equatorial boundary based view-line, $P(A)_{max}$ was below the threshold of
350 18%. Whilst this is unfortunate, the number of reports remaining for each comparison is
351 still significant.

6. Conclusion

352 More than sixty years ago *Gartlein and Moore* [1951] showed that dedicated amateur
353 observers could make critical contributions to some of the earliest auroral models and now,
354 as shown in this study, observers armed with modern mobile crowdsourcing technologies
355 are making demonstrable improvements to the latest models too.

356 Specifically, in this study, citizen science reports of auroral visibility (or lack thereof),
357 provided by the Aurorasaurus project, were compared to an updated version of NOAA's
358 SWPC OVATION Prime based view-line. The reports consist of positive sightings and
359 negative reports submitted directly to Aurorasaurus, along with verified tweets, which are
360 positive sightings reported on Twitter and verified by Aurorasaurus users. The reports
361 were collected during March and April 2015 and covered a range of latitudes, local time,
362 and geomagnetic activity.

363 The reports demonstrated that, during these two months, the updated SWPC view-
364 line under-estimated the distance from which an aurora could be observed. Over 60%
365 of the positive reports (which includes positive sightings and verified tweets) occurred
366 at latitudes equatorward of the view-line. The accuracy (Equation 3) was found to be
367 poor at just under 44% (though, as previously discussed, there are several caveats to

368 this accuracy value). These results suggested that further investigation into the scaling
369 parameters used in the SWPC view-line calculation (Equation 2) was warranted.

370 New scaling parameters for the view-line equation were determined from the relationship
371 of the differences in latitude between the positive reports and the updated SWPC view-
372 line, and the maximum probability of visible aurora. This modified Aurorasaurus view-
373 line takes a very similar form to the updated SWPC view-line but scales the line further
374 equatorward. With these modified parameters, nearly 93% of the positive reports occurred
375 at latitudes poleward of the view-line. The accuracy drastically improved and, in fact,
376 more than doubled to 91%.

377 The updated SWPC view-line, and the modified Aurorasaurus version of it, scale the
378 latitude of the maximum probability of visible aurora. As discussed, this may not always
379 be the most appropriate location to scale. Therefore a view-line based upon the location
380 of the auroral equatorial boundary was also constructed. This view-line also performed
381 well, and slightly better than the Aurorasaurus view-line, with 97% of the positive reports
382 occurring poleward of the view-line and the overall accuracy of 95%. Though the restric-
383 tion placed on when the view-line should be drawn (i.e. $P(A)_{max}$) resulted in comparisons
384 with fewer reports.

385 Of course, it should be expected that view-lines created using a set of observations
386 should perform well when then compared to those observations. It is therefore sensible
387 to test these view-lines (Equations 2, 4 and 5) further using other data and adapt them
388 as necessary. For example, the Aurorasaurus data set has aurora observations spanning
389 from November 2014 to present. Further work to incorporate those observations seems
390 a worthwhile endeavor. We note, however, that the equatorial based view-line has been

391 running on the Aurorasaurus website since November 2015 and, anecdotally, has matched
392 well with the reports from citizen scientists that have been submitted since then (including
393 those submitted during a few large auroral events).

394 We note that, in this case study, there was a limited number of negative reports which
395 resulted in the accuracy of the view-lines being predominantly determined by how well
396 they were able to predict true positives. Additionally, reports were generally provided by
397 observers located on the equatorward edge of a visible aurora. As a result the view-lines
398 created in this study may sometimes overestimate the distance from which the aurora can
399 be seen and so should be treated as the most optimistic values. Ideally, the number of
400 useful negative reports (whereby a user has a clear sky but is unable to view the aurora)
401 should roughly equal the number of positive reports and the reports should span right
402 across the auroral oval. Future studies should aim to address these issues.

403 Additionally, it is important to note that the view-lines used in this case-study are based
404 upon the output of the OP13 model. Although this model has shown to be accurate at
405 modeling the extent of the auroral oval, at least statistically, there may be times when
406 it does not perform quite so well (e.g. during substorms [*Newell et al.*, 2010a; *Machol et*
407 *al.*, 2012]) or the real-time aurora is not quite as expansive as suggested. It is also unable
408 to make any estimates as to the height or color of the aurora which are both factors that
409 may significantly affect where an aurora can be seen from [*Machol et al.*, 2012]. Improving
410 the modeling of the aurora, and the conversion of energy flux to SWPC's "probability of
411 visible aurora" (by taking local time into account, for example), will therefore improve
412 the accuracy of any view line. Using the Aurorasaurus reports to help account for such

413 factors may improve the accuracy of OVATION Prime and, subsequently, any view-lines
414 based upon it.

415 Lastly, in this case study, the three view-lines discussed were all estimates of the equa-
416 torial extent of auroral visibility. In principle, the poleward extent of visible aurora could
417 also be determined. The poleward view-line could use either the same scaling parameters
418 discussed here or, more ideally, new scaling parameters could be determined. In practise,
419 such determination might prove more difficult due to a lack of citizen science reports at
420 extremely high latitudes. Further work might attempt to mitigate this issue, perhaps
421 using automated camera observations, to provide a view-line for even the most poleward
422 of observers.

423 **Acknowledgments.** This material is based upon work supported, in part, by the
424 National Science Foundation (NSF) under Grant #1344296. Any opinions, findings, and
425 conclusions or recommendations expressed in this material are those of the author(s) and
426 do not necessarily reflect the views of NSF.

427 The OVATION Prime output and associated view-line were kindly supplied by the
428 Space Weather Prediction Center, Boulder, CO, National Oceanic and Atmospheric Ad-
429 ministration (NOAA), US Dept. of Commerce. The output can be freely downloaded
430 from the NOAA SWPC product pages ([http://www.swpc.noaa.gov/products/aurora-30-](http://www.swpc.noaa.gov/products/aurora-30-minute-forecast)
431 [minute-forecast](http://www.swpc.noaa.gov/products/aurora-30-minute-forecast)).

References

432 Bartels, J., N. H. Heck, and H. F. Johnston (1939), The three-hour-range in-
433 dex measuring geomagnetic activity, *Terr. Magn. Atmos. Electr.*, *44*(4), 411-454,

- 434 doi:10.1029/TE044i004p00411
- 435 Baumgardner, J., J. Wroten, J. Semeter, J. Kozyra, M. Buonsanto, P. Erickson, and
436 M. Mendillo (2008), A very bright SAR arc: implications for extreme magnetosphere-
437 ionosphere coupling, *Annales Geophysicae*, *25*(12), 2593–2608, doi:10.5194/angeo-25-
438 2593-2007
- 439 Case, N. A., E. A. MacDonald, M. Heavner, A. H. Tapia, and N. Lalone (2015a),
440 Mapping auroral activity with Twitter, *Geophys. Res. Lett.*, *42*, 3668–3676. doi:
441 10.1002/2015GL063709.
- 442 Case, N. A., E. A. MacDonald and K. G. Patel (2015b), Aurorasaurus and the St Patrick’s
443 Day storm, *Astronomy & Geophysics*, *56*(3), 3.13–3.14, doi: 10.1093/astrogeo/atv089.
- 444 Donovan, E., Spanswick, E., Liang, J., Grant, J., Jackel, B. and Greffen, M. (2012)
445 Magnetospheric Dynamics and the Proton Aurora, in *Auroral Phenomenology and*
446 *Magnetospheric Processes: Earth And Other Planets*, (eds A. Keiling, E. Donovan,
447 F. Bagenal and T. Karlsson), American Geophysical Union, Washington, D. C.. doi:
448 10.1029/2012GM001241
- 449 Hardy, D. A., M. S. Gussenhoven, and E. Holeman (1985), A statistical
450 model of auroral electron precipitation, *J. Geophys. Res.*, *90*(A5), 4229–4248,
451 doi:10.1029/JA090iA05p04229.
- 452 Hardy, D. A., M. S. Gussenhoven, and D. Brautigam (1989), A statistical model of auroral
453 ion precipitation, *J. Geophys. Res.*, *94*(A1), 370–392, doi:10.1029/JA094iA01p00370.
- 454 Gartlein, C. W., and R. K. Moore (1951), Southern extent of Aurora Borealis in North
455 America, *J. Geophys. Res.*, *56*(1), 85–96, doi:10.1029/JZ056i001p00085.

- 456 Kataoka, R., Y. Miyoshi, K. Shigematsu, D. Hampton, Y. Mori, T. Kubo, A. Yamashita,
457 M. Tanaka, T. Takahei, T. Nakai, H. Miyahara, and K. Shiokawa (2013), Stereoscopic
458 determination of all-sky altitude map of aurora using two ground-based Nikon DSLR
459 cameras, *Annales Geophysicae*, *31*(9), 1543–1548, doi:10.5194/angeo-31-1543-2013
- 460 Lane, C., A. Acebal, and Y. Zheng (2015), Assessing predictive ability of three au-
461 roral precipitation models using DMSP energy flux, *Space Weather*, *13*, 61–71,
462 doi:10.1002/2014SW001085.
- 463 MacDonald, E. A., N. A. Case, J. H. Clayton, M. K. Hall, M. Heavner, N. Lalone, K. G.
464 Patel, and A. Tapia (2015), Aurorasaurus: A citizen science platform for viewing and
465 reporting the aurora, *Space Weather*, *13*, doi:10.1002/2015SW001214.
- 466 Machol, J. L., J. C. Green, R. J. Redmon, R. A. Viereck, and P. T. Newell (2012),
467 Evaluation of OVATION Prime as a forecast model for visible aurorae, *Space Weather*,
468 *10*, S03005, doi:10.1029/2011SW000746.
- 469 Mitchell, E. J., P. T. Newell, J. W. Gjerloev, and K. Liou (2013), OVATION-SM: A model
470 of auroral precipitation based on SuperMAG generalized auroral electrojet and substorm
471 onset times, *J. Geophys. Res. Space Physics*, *118*, 3747–3759, doi:10.1002/jgra.50343.
- 472 Newell, P. T., T. Sotirelis, K. Liou, C.-I. Meng and F. J. Rich (2007), A nearly univer-
473 sal solar wind-magnetosphere coupling function inferred from 10 magnetospheric state
474 variables, *J. Geophys. Res.*, *112*, doi:10.1029/2006JA012015.
- 475 Newell, P. T., T. Sotirelis, K. Liou, A. R. Lee, S. Wing, J. Green, and R. Redmon (2010),
476 Predictive ability of four auroral precipitation models as evaluated using Polar UVI
477 global images, *Space Weather*, *8*, S12004, doi:10.1029/2010SW000604.

- 478 Newell, P. T., T. Sotirelis, and S. Wing (2010), Seasonal variations in dif-
479 fuse, monoenergetic, and broadband aurora, *J. Geophys. Res.*, *115*, A03216,
480 doi:10.1029/2009JA014805.
- 481 Newell, P. T., K. Liou, Y. Zhang, T. Sotirelis, L. J. Paxton, and E. J. Mitchell (2014),
482 OVATION Prime-2013: Extension of auroral precipitation model to higher disturbance
483 levels, *Space Weather*, *12*, 368–379, doi:10.1002/2014SW001056.
- 484 Poppe, B. B. (2000), New scales help public, technicians understand space weather, *Eos*
485 *Trans. AGU*, *81*(29), 322–328, doi:10.1029/00EO00247.
- 486 Roble, R. G., and E. C. Ridley (1987), An auroral model for the NCAR thermospheric
487 general circulation model (TGCM), *Annales Geophysicae*, *5*, 369–382.
- 488 Sequeira, A. M., P. E. Roetman, C. B. Daniels, A. K. Baker and C. J. Bradshaw (2014),
489 Distribution models for koalas in South Australia using citizen science collected data,
490 *Ecology and evolution*, *4*(11), 2103–2114, doi: 10.1002/ece3.1094.
- 491 Spiro, R. W., P. H. Reiff, and L. J. Maher Jr. (1982), Precipitating electron energy flux and
492 auroral zone conductances-An empirical model, *J. Geophys. Res.*, *87*(A10), 8215–8227,
493 doi:10.1029/JA087iA10p08215.
- 494 Zhang, Y., and L. J. Paxton (2008), An empirical Kp-dependent global auroral model
495 based on TIMED/GUVI FUV data, *Journal of Atmospheric and Solar-Terrestrial*
496 *Physics*, *70*(8–9), 1231–1242, doi:10.1016/j.jastp.2008.03.008.

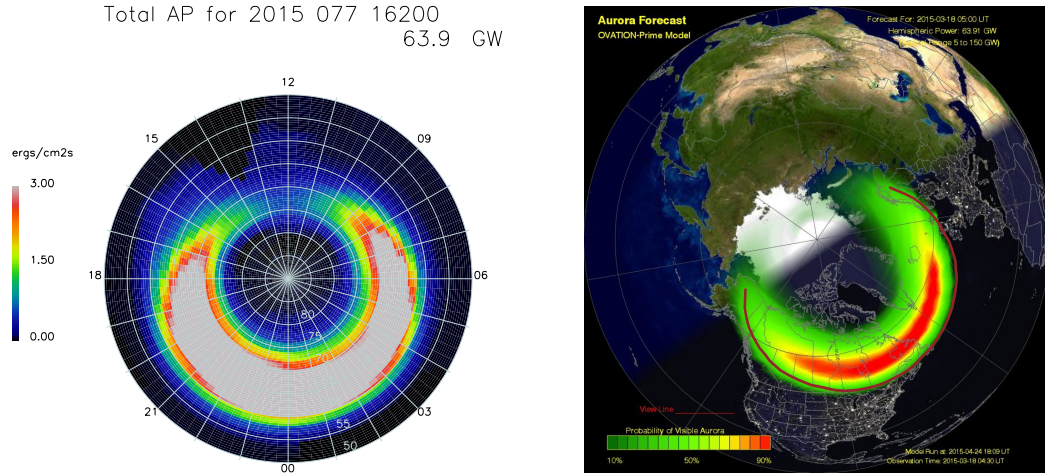


Figure 1. (left) The OVATION Prime (2013) auroral precipitation output, in terms of energy flux, in geomagnetic coordinates (04:30 UT on 18 March 2015). (right) The updated SWPC output, in terms of visible aurora probability, in geographic coordinates using the same OP13 data.

Table 1. A summary of the view-lines and their accuracies

View-line	Equation	Accuracy (%)
Updated SWPC	$\phi_{VL}^{SWPC} = \phi_{P(A)max} \pm \left(\frac{P(A)_{max}}{20} + 3 \right)$	43.9
Aurorasaurus	$\phi_{VL}^{AS} = \phi_{P(A)max} \pm \left(\frac{P(A)_{max}}{16} + 8 \right)$	90.1
Equatorial Boundary	$\phi_{VL}^{EB} = \phi_{EB} \pm 8$	91.2

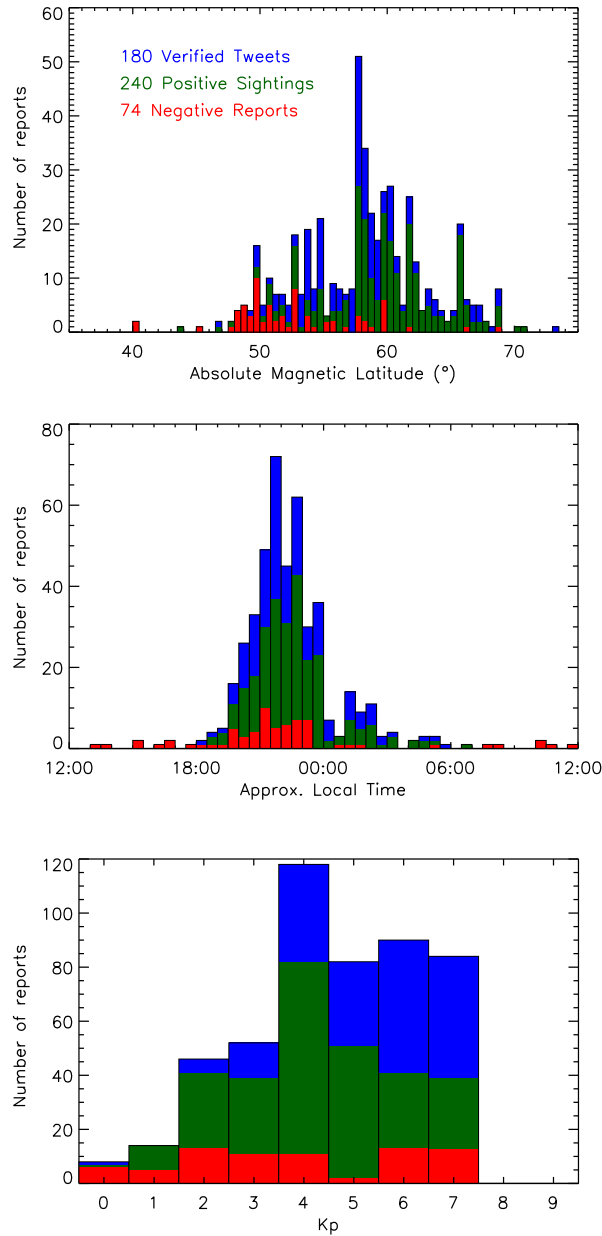


Figure 2. Histograms of the Aurorasaurus reports, submitted during March and April 2015, grouped by (top) absolute magnetic latitude (in 0.5° bins), (middle) approximate local time (30min bins), and (bottom) Kp index at the start of the report. The stacked red bars indicate negative reports, the green bars indicate positive sightings and the blue bars indicate verified positive reports posted on Twitter, known as verified tweets.

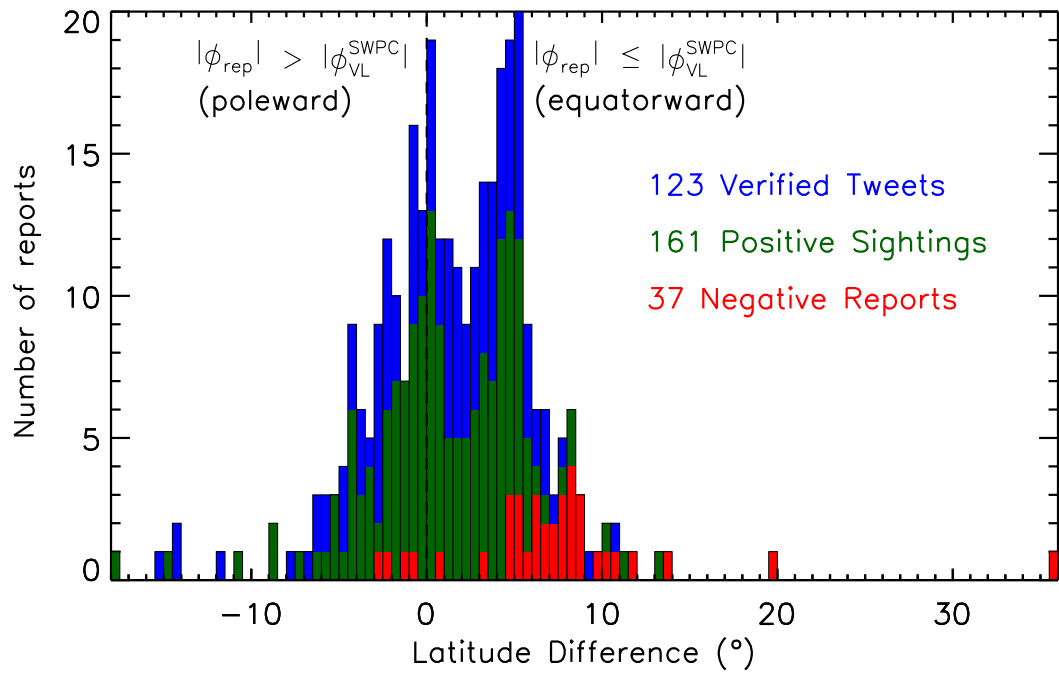


Figure 3. A histogram of the differences in latitude between the Aurorasaurus reports (ϕ_{rep}) and the updated SWPC view-line (ϕ_{VL}^{SWPC}). The differences are grouped in 0.5° intervals and the stacked bars indicate the number of each type of report in each interval. The red bars indicate negative reports, the green bars indicate a positive sightings and the blue bars indicate verified tweets.

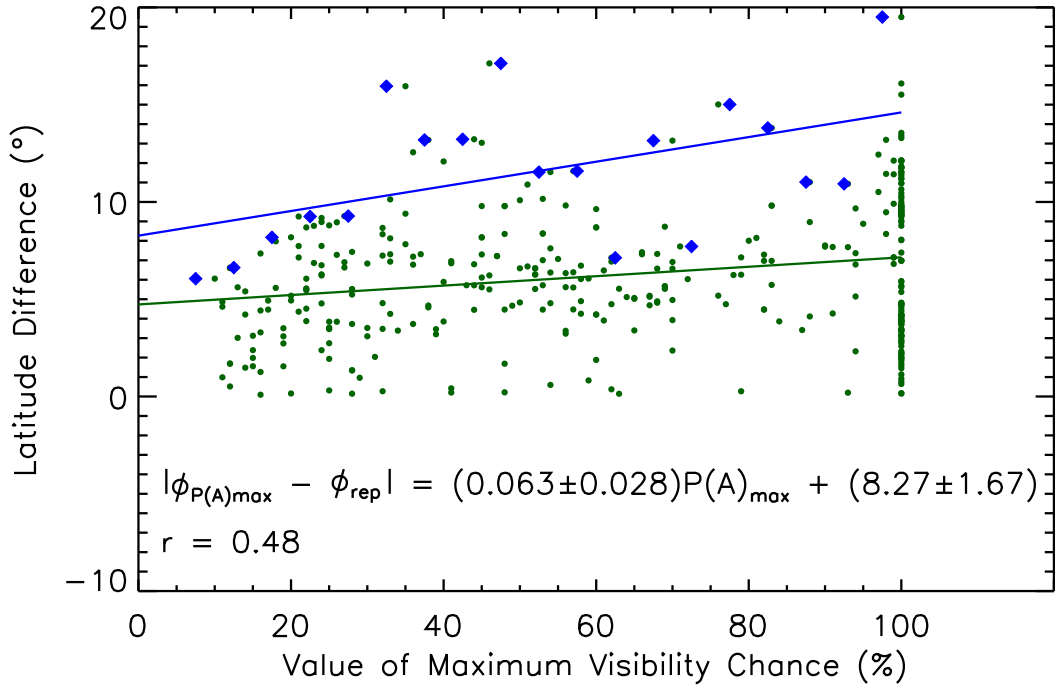


Figure 4. The latitude difference between the positive reports and the location of maximum visibility (i.e. $|\phi_{P(A)_{\max}}| - |\phi_{\text{rep}}|$), plotted as a function of the maximum visibility ($P(A)_{\max}$). The data are filtered to positive reports with positive differences (i.e. $|\phi_{P(A)_{\max}}| > |\phi_{\text{rep}}|$). The solid green line is the least squares fit through all of the data and the solid blue line is the least squares fit through the maximum difference in each 5° bin (represented by blue diamonds). The fit equation shown is for the blue line.

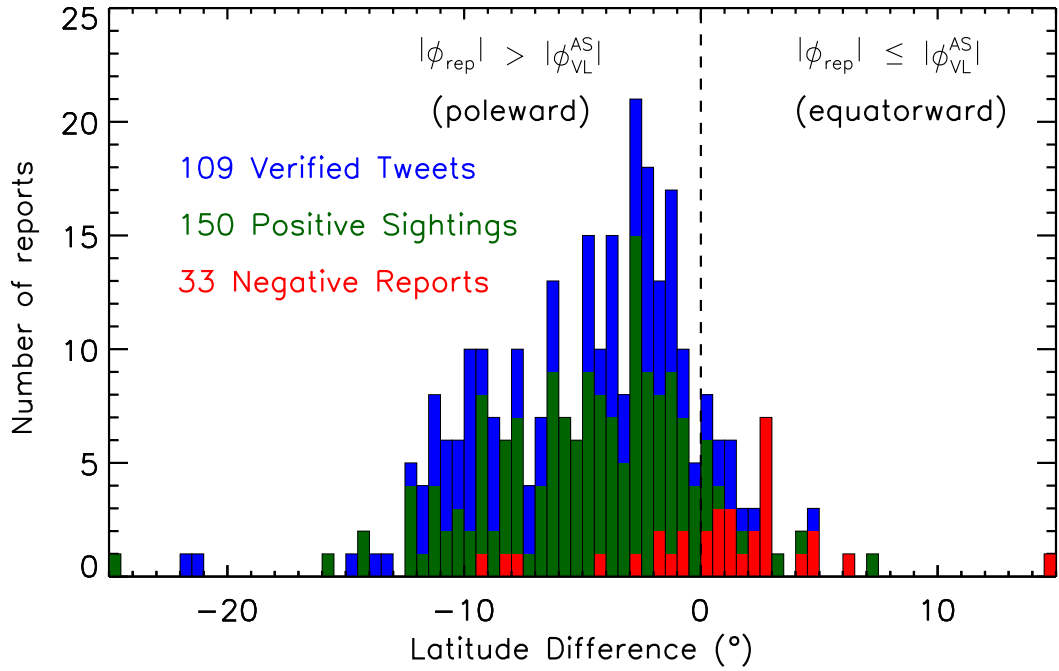


Figure 5. Of the same form as Figure 3. A histogram of the differences in latitude between the Aurorasaurus reports (ϕ_{rep}) and the Aurorasaurus view-line (ϕ_{VL}^{AS}).

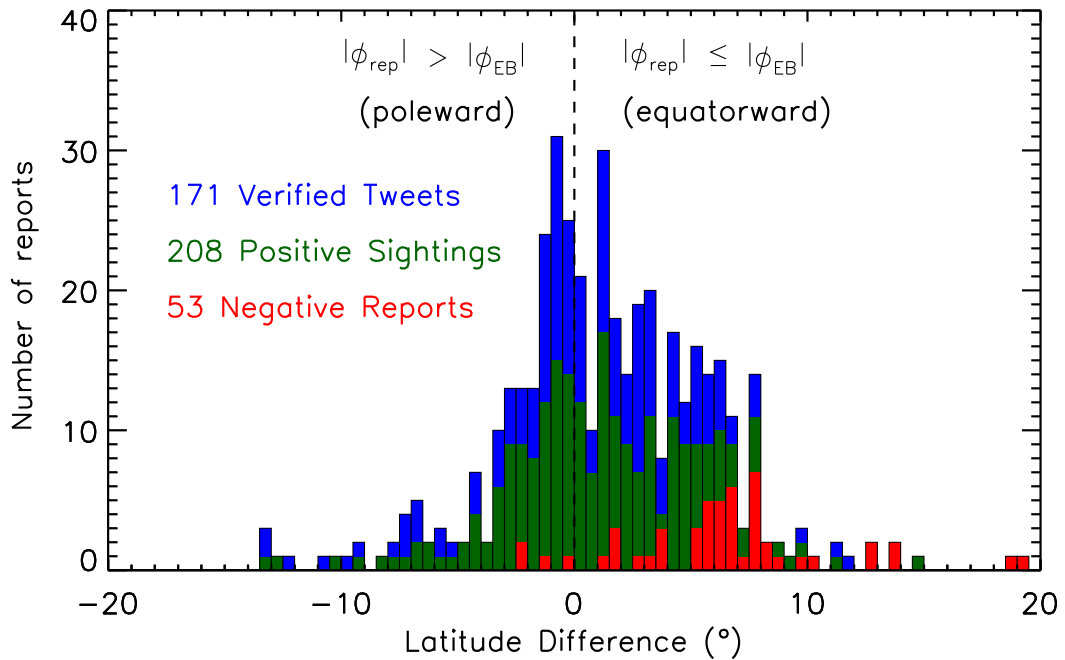


Figure 6. Of the same form as Figure 3. A histogram of the differences in latitude between the Aurorasaurus reports (ϕ_{rep}) and the auroral oval equatorial boundary (ϕ_{EB}).

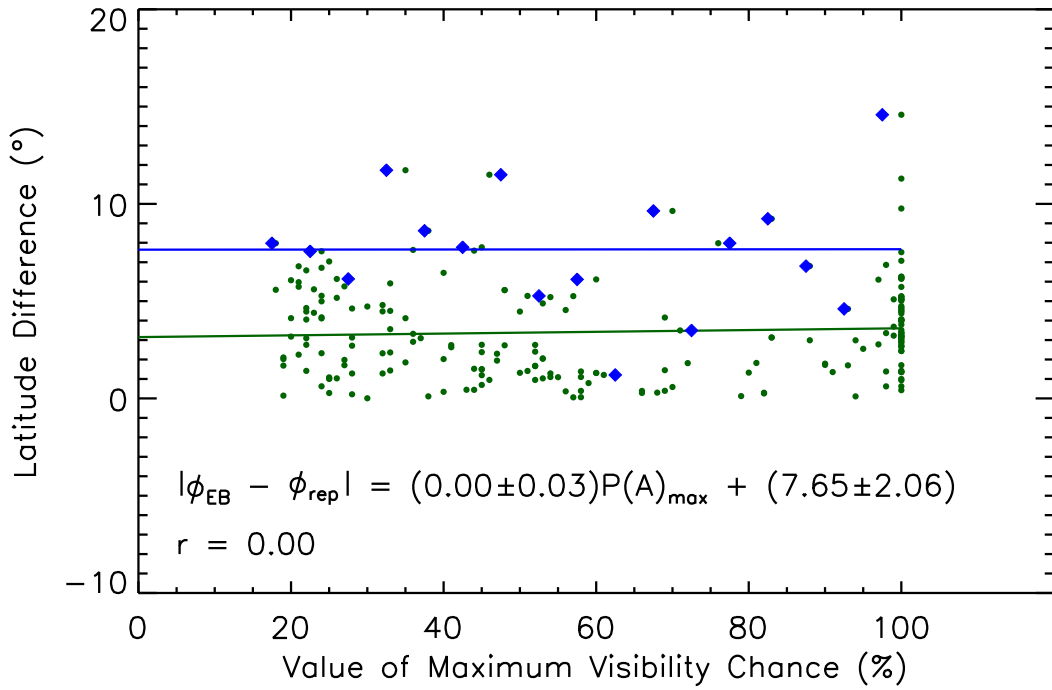


Figure 7. Of the same form as Figure 4. The latitude difference between the positive reports and the equatorial boundary ($|\phi_{EB}| - |\phi_{rep}|$) is plotted as a function of the maximum visibility ($P(A)_{max}$).

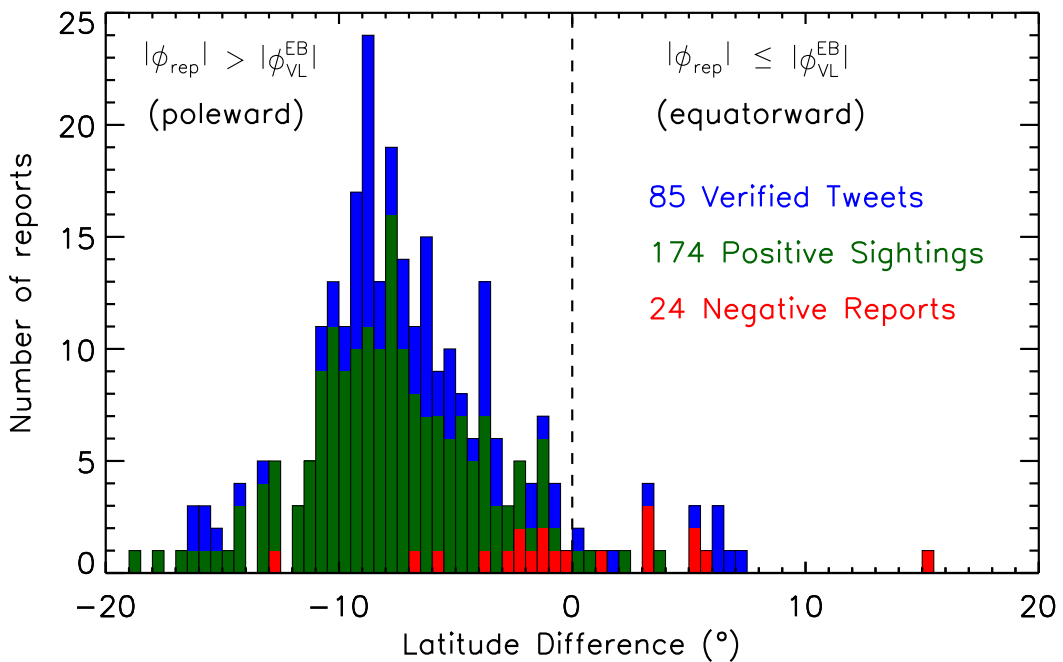


Figure 8. Of the same form as Figure 3. A histogram of the differences in latitude between the Aurorasaurus reports (ϕ_{rep}) and the equatorial boundary based view-line (ϕ_{VL}^{EB}).